Soil erosion susceptibility assessment of Swat River sub-watersheds using the morphometry-based compound factor approach and GIS

Muhammad Jamal Nasir
University of Peshawar
Waqas Ahmad (wahmad.ms17igis@igis.nust.edu.pk)
National University of Science and Technology, IGIS
Changhyun Jun
Chung-Ang University
Javed Iqbal
National University of Science and Technology, IGIS

Research Article

Keywords: Morphometry, compound factor, soil erosion susceptibility, watershed prioritization, Swat River watershed

Posted Date: December 8th, 2022

DOI: https://doi.org/10.21203/rs.3.rs-2344750/v1

Additional Declarations: No competing interests reported.

Version of Record: A version of this preprint was published at Environmental Earth Sciences on June 7th, 2023. See the published version at https://doi.org/10.1007/s12665-023-10982-4.

Abstract

Watershed prioritization is essential in sub-watershed (SW) natural resource management. The Swat River watershed in the Hindukush mountains of Pakistan's Khyber Pakhtunkhwa province covers an area of 5337 km2. Using an Advanced Spaceborne Thermal Emission and Reflection Radiometer digital elevation model with a resolution of 30 m obtained from the United States Geological Survey (USGS), the present study identified 17 SWs (SW1–17) with drainage patterns ranging from dendritic to sub-dendritic in nature. The SWs were assessed for their susceptibility to erosion via GIS-based assessment using a morphometry-based compound factor (CF) approach. A total of 15 linear, aerial, and relief morphometric characteristics were identified and analyzed. The SWs were ranked for each morphometric parameter based on its contribution to the erodibility of the SW. A ranking of 1 indicated that the SW had the greatest susceptibility to erosion for that parameter and a ranking of 17 indicates that it had the lowest. These rankings were summed to calculate the CF, which thus indicated the combined influence of these characteristics on the erosion susceptibility of the SW (a lower CF indicated a higher susceptibility to erosion). The SWs were consequently divided into four groups based on their susceptibility to erosion using the calculated CF: very high, high, moderate, and low susceptibility. SW8, SW12, and SW15 had the lowest CFs (8.0, 8.9, and 8.9, respectively) and were thus extremely vulnerable to erosion. In contrast, SW1, SW2, and SW4 had the highest CFs (13.4, 13.8, and 11.8, respectively) and were the least vulnerable to erosion. The very high-priority SWs were characterized by the presence of fifth-order streams, a length of overland flow of 1.20–1.61, a very high basin relief of 1720–2937, the highest relief ratio of 102.10–205.24, a low shape factor of 1.51–2.67, and a farm factor of 0.37–0.66. The present study demonstrates that the key morphometric characteristics that impact soil erosion are basin form and relief parameters, such as the basin relief and relief ratio. This study illustrates that the CF approach to determining the susceptibility of SWs to soil erosion is extremely valuable for planners and decision-makers for soil conservation efforts at the SW level.

1. Introduction

Soil and water are considered the two most important natural resources for both human subsistence and the social and economic development of a region (Debelo et al., 2017). Soil is a finite resource that is vital for food production, carbon sequestration, biodiversity enhancement, and water and climate regulation (Arshad and Martin, 2002). Thus, soil degradation is regarded as a severe global environmental concern (Powlson et al., 2011; Pimental and Burgess, 2013), particularly given the need to feed a rapidly growing global population. Soils globally are subject to both natural degradation processes affected by the climate (e.g., rainfall volume, frequency, intensity, and duration), soil type, slope, and terrain (Ghabbour et al., 2017) and anthropogenic effects associated with rapid population growth, economic development, changing climatic patterns, land cover changes, inappropriate land use, and inadequate land management (Keesstra et al., 2016).

Soil erosion is the removal and transfer of the Earth's top layer via mobile geomorphic processes such as water, wind, and glaciers. Of these agents, water has the highest impact on soil erosion; the UNEP (1997) reported that human-induced soil degradation had affected 1.964 billion ha worldwide, of which 1.903 billion ha was due to the action of water and 0.548 billion ha to the action of wind. According to a recent estimate by Borrelli et al. (2017), the potential annual loss of soil is 35 Pg yr^{-1}, with a worldwide increase in soil erosion of 0.86 Pg yr^{-1} (2.5%) between 2001 and 2012, mostly due to agricultural expansion and land cover changes. Soil erosion is also expected to increase at the highest rates in Sub-Saharan Africa, South America, and Southeast Asia.

To prevent soil erosion, it is important to locate the primary sources of sediment production and identify the watershed characteristics that are indicative of these sources. This is because the primary mechanism of sediment generation and transport into the fluvial system is soil erosion caused by a range of geomorphic processes. By locating these sources and identifying the indicators, those watersheds that require immediate intervention via sediment control management to avert soil loss can be prioritized. The primary method of transit for sediment in streams is via suspended load (Hillier, 2000), with

reservoirs often the final resting place for the silt created by soil erosion. This process reduces the storage capacity of reservoirs (Eroglu et al., 2010; Vaezi et al., 2017; Tundu et al., 2018), with an annual loss of storage capacity of around 0.5% to 1% due to reservoir sedimentation (Chuenchum et al., 2020). At this rate, it is anticipated that, by 2050, many reservoirs worldwide will have lost half of their current capacity. In addition, Walling (2011) reported that sedimentation has reduced the storage capacity of reservoirs by 40% in Asia.

Warsak Dam was erected on the Kabul River in Pakistan's Khyber Pakhtunkhwa province, 30 km northwest of Peshawar. It was the first project of its kind after Pakistan's independence, and it cost PKR 394.98 million to complete in 1960. However, the resulting reservoir silted up after only three years of operation, dramatically reducing its water storage capacity. De-silting the reservoir is not an option because doing so would cost more than building a new dam. In addition, the water flow into the reservoir increases by 50% from April to September, leading to the transport of large volumes of abrasive debris, thus causing the turbines to wear out rapidly (Sabir et al., 2013; Duarte, 2019).

Several methodologies have been developed for the assessment of soil erosion and sediment output, including directly quantitative approaches and those based on watershed prioritization using geomorphometric factors. Some of the most significant of these techniques include the Hybrid Computational Intelligence Model (Arabameri et al., 2020), Revised Universal Soil Loss Equation (RUSLE) (Mohammad et al., 2020; Chuenchum et al., 2020), Universal Soil Loss Equation (USLE) (Maqsoom et al., 2020), Integrated Universal Soil Loss Equation (Pham et al., 2018), Chemical, Runoff and Erosion from Agriculture Management System (CREAMS) (Rekolainen and Posch, 1993), Ephemeral Gully Erosion Model (EGEM) (Gudino et al., 2018; Karydas and Panagos, 2020), Erosion Productivity Impact Calculator (EPIC) (Tan and Shibasaki, 2003), European Soil Erosion Model (EUROSEM) (Berberoglu et al., 2020), Groundwater Loading Effect of Agricultural Management Systems (GLEAMS) (DeMars et al., 2018), Instituto Nacional Para La Conservacion De La Naturaleza (ICONA) model (Bayramin et al., 2003; Esmaeili et al., 2020), Water Erosion Prediction Project (WEPP) (Brooks et al., 2016), weight of evidence and evidential belief function (Gayen and Saha, 2017), and morphometry-based compound factor (CF) approach (Hembram and Saha, 2020; Sadasivam et al., 2020; Jothimani et al., 2020).

Watershed prioritization has recently been facilitated by advances in Geographic Information System (GIS) and remote sensing (RS) technology (Chen et al., 2020; Mundetia et al., 2018). These technologies, combined with machine-learning methodologies, produce promising results when modeling natural resources (Avand et al., 2020; Hosseini et al., 2020). In particular, machine learning has been shown to outperform traditional techniques in the assessment of the risk of soil erosion (Mosavi et al., 2020a; Amiri and Pourghasemi, 2020). This soil erosion risk assessment helps to clearly identify vulnerable regions so that soil erosion management plans can be devised and implemented (Azareh et al., 2019; Mosavi et al., 2020b). The current study thus aims to identify sub-watersheds (SWs) vulnerable to soil erosion in the Swat River watershed using the geomorphometric CF approach. The findings will be useful in preserving valuable land and water resources within the watershed.

2. Study Area

Swat River watershed, also known as the Swat Valley, is part of the Swat district, which is a high-altitude region in the Hindukush mountains of Pakistan's Khyber Pakhtunkhwa province. Geographically, it is located at a latitude of 34°31'45" to 35°52'25" N and a longitude of 72°05'02" to 72°45' 20" E. The Swat district is bordered by Dir in the west, Malakand district in the south, Buner in the southeast, Shangla in the east, Gilgit Baltistan in the north, Kohistan in the northeast, and Chitral in the northwest. According to the 2017 census, it had a total population of 2.309 million people and a total area of 5337 km^2 (GoP, 2018). It connects China to Central Asia and Europe. Swat was a prominent hub for Gandharan Buddhism and Hinduism until the 10th century (Vidale and Olivieri, 2002). The Swat district was an autonomous state until 1969, when it was annexed by Pakistan. The length of the Swat Valley is 146 km, with the width of the valley averaging 30–35 km. The main river in the study area is the Swat River, which flows from the confluence of the Ushu and Gabral Rivers in the Kalam Valley and is fed by glacier melt and springs. It flows for 160 km from north to south, joining the Panjkora River in Qalangi

and eventually emptying into the Kabul River at Charsadda. The Swat River basin is split into 17 SWs (Nasir et al., 2020). The Daral, Gabral, Lalkoo, and Harnoi Streams are key western tributaries, while the Ushu and Beshigram Streams are important eastern tributaries. Swat means “pure water” in Sanskrit, and the river is also known as Suvastu in Reg Veda (Shah et al., 2016).

3. Methods

3.1 Data and GIS analysis

The primary data source for the present study was an Advanced Spaceborne Thermal Emission and Reflection Radiometer (ASTER) digital elevation model (DEM) with a resolution of 30 m acquired from the United States Geological Survey (USGS). This study uses geospatial modeling and morphometric analysis of the Swat River watershed to identify its physical features and explain the soil erosion processes in the SWs. The SWs were delineated using Arc Hydro software and the DEM, which provided a reasonable depiction of the topography (Waikar and Nilawar, 2014). The DEM was processed to extract various drainage basin parameters such as the slope and drainage network (Wakode et al., 2013; Buccolini et al., 2012).

To increase the accuracy of the DEM for stream network extraction, sinks were removed from the data using Arc Hydro. Sinks are groups of cells that have the same height, generating gaps in the DEM and disrupting cell communication. A flow accumulation grid was created from a flow direction grid, while a threshold area of 1%, which has been recommended by Martins and Giga (2015) and Azizian and Shokoohi (2015), was utilized to extract the stream network from the flow accumulation grid. This form of GIS- and DEM-based parameterization of a watershed offers a rapid approach to morphometric analysis (Grohmann et al., 2007; Kacem et al., 2006).

3.2 Morphometric parameterization

In the present study, the morphometric characteristics used to identify the SWs susceptible to erosion were the stream number, stream order, stream length, bifurcation ratio, drainage density, stream frequency, length, width, length–width ratio, texture ratio, shape factor, circulatory ratio, elongation ratio, and drainage texture. Table 1 presents the linear and aerial morphometric parameters and their mathematical formulas. The stream order was determined using the Strahler (1964) system due to its simplicity and extensive use in morphometric research. In Strahler's system, the smallest unbranched tributary is classified as a first-order stream and, when two first-order streams merge, they become a second-order stream. The trunk stream, which is supplied by multiple-order streams, is a basin's highest-order stream. The number of streams in each order was tallied and their length recorded. The Arc Hydro extension of Arc Map 10.5.2 was used to calculate the morphometric characteristics and subsequently determine the susceptibility of the SWs to erosion using the process illustrated in Fig. 2, which was adapted from Hembram and Shah (2020).

Table 1. Morphometric parameters and their mathematical formulas (compiled from Horton, 1945; Smith, 1950; Strahler, 1964; Cutter, 2008; and Rahaman et al., 2015).

S.No	Morphometric Parameters			Formulas/Definitions	References
1	Linear	Stream Order (u)	Group 1	Hierarchical rank	Strahler (1964)
2		Stream Number (Nu)		Number of streams	
3		Stream Length (Lu)		Length of stream (km)	Horton (1945)
4		Bifurcation Ratio (Rb)		$Rb = \frac{Nu}{Nu} + 1$ Rb=bifurcation ratio Nu=total number of stream segments Nu+1= number of streams in next higher order	Schumms (1956)
5	Relief parameter	Length of Overland Flow		$Lg = \frac{1}{D} \square 2$ Lg=length of overland flow D=drainage density	Horton (1945)
6		Basin Relief (Bh)		$Bh = H - h$ Bh=basin relief H=maximum relief and h=minimum relief	Horton (1945)
7		Relief Ratio (Rr)		$Rr = Bh / Lb$ Rr=relief ratio Bh= basin relief (maximum-minimum relief) Lb=basin length	Horton (1945)
8	Aerial Parameters	Drainage Density (Dd)		$D = \frac{Lu}{A}$ D=drainage density A= basin area (km^2)	Horton (1932)
9		Drainage Frequency (Fs)		$Fs = \frac{Nu}{A}$ Fs= drainage frequency A= basin area (km^2)	Horton (1932)
10		Drainage Texture (Rt)		$Rt = \frac{Nu}{P}$ Rt= drainage texture Nu=total no. of stream of all orders P=perimeter of the basin (km)	Horton (1945)
11		Farm Factor	Group 2	$Rf = A / Lb^2$ Rf = form factor A=basin area (km^2) Lb^2=square of the basin length	Horton (1932)
12		Shape Factor		Lb^2 / A Lb^2=square of the basin length A=basin area (km^2)	Gregory and Walling (1973)
13		Circulatory Ratio		$Rc = 4\pi \times A / P^2$ π=3.14 A=Basin Area (km^2) P=Perimeter (km)	Miller (1953)
14		Elongation Ratio		$\square = (2Lb)\sqrt{(\frac{A}{\pi})}$ Re= elongation ratio A=basin area (km^2) π=3.14 Lb=basin length	Schumms (1956)
15		Compactness Coefficient		$Cc = P / Pu$ Cc= compactness coefficient P= watershed perimeter Pu= perimeter of the circle of the watershed area	Horton (1945)

3.3 Integrating watershed morphometry and erosion susceptibility assessment

Variation in a watershed's geomorphometric parameters impact the prevalence of soil erosion, thus these parameters are widely used to determine susceptibility to soil erosion (Bhattacharia et al., 2020). This susceptibility for the 17 SWs in the Swat River watershed was evaluated analytically with GIS/RS by quantifying the morphometric characteristics and processes and using them to rank the SWs according to the potential risk of erosion. Geomorphometric parameters can be classified into two groups based on their geomorphometric properties and their contribution to the potential soil erosion risk. Group 1 includes parameters that have a positive association with soil erosion, which means that the higher the value of these parameters, the greater the risk of erosion (Kadam et al., 2019). This group includes the drainage density, drainage frequency, bifurcation ratio, drainage texture, length of overland flow, and basin relief. Group 2, on the other hand, includes geomorphometric parameters that are negatively associated with soil erosion, i.e., the higher their value, the lower the risk of erosion. Group 2 comprises basin form factors such as the farm factor, circulatory ratio, and elongation ratio. These parameters are summarized in Tables 2 and 3.

Table 2. Basic and landscape attributes for the Swat River sub-watersheds (SWs)

SWs	Basin Area (km^2)	Perimeter (km)	Max. Elevation (m)	Min. Elevation (m)	Difference in Elevation (m)	Perimeter of the circle of the watershed (km)	Basin Length (km)	Longest Flow Path (km)	Gradient/km
SW1	1221.2	202.27	5856	1959	3897	177.11	60.91	49.80	78.25
SW2	789.71	182.40	5946	1953	3993	193.78	55.88	47.77	83.59
SW3	271.15	82.84	4823	1406	3417	59.42	24.69	24.32	140.50
SW4	181.48	61.87	5707	1677	4030	81.36	15.50	16.11	250.16
SW5	153.62	60.50	3992	1235	2757	40.53	18.22	22.19	124.25
SW6	433.92	110.57	4071	1033	3038	54.04	32.28	36.03	84.32
SW7	76.33	40.07	4607	1579	3028	61.20	10.66	13.86	218.47
SW8	146.30	53.59	4296	1359	2937	41.60	14.86	14.31	205.24
SW9	63.67	37.15	3517	1262	2255	33.08	12.21	14.88	151.55
SW10	190.74	71.96	2883	859	2024	114.15	20.25	22.22	91.09
SW11	155.99	55.40	2794	777	2017	48.24	12.16	12.08	166.97
SW12	104.62	49.13	2779	1077	1702	83.17	13.09	16.67	102.10
SW13	204.66	71.05	3003	952	2051	71.76	13.91	19.93	102.91
SW14	15.92	20.41	1495	720	775	44.12	4.16	5.03	154.08
SW15	37.53	27.48	3137	1235	1902	24.21	10.01	10.53	180.63
SW16	55.34	41.61	1892	742	1150	69.01	7.90	11.71	98.21
SW17	274.03	80.31	3002	882	2120	54.76	22.23	24.16	78.25

Table 3. Linear, aerial, and relief morphometric parameters for the Swat River SWs.

SWs	Linear					Relief		Aerial Parameters							
	U	Nu	Rb	R_L	Lg	Bh	Rr	Dt	Dd	Fs	Cc	Rc	Re	Bs	Rf
	Group 1										GROUP 2				
SW1	6	2511	4.58	1.271	1.31	3897	78.25	12.41	1.53	2.05	1.14	0.40	0.31	3.04	0.33
SW2	6	1597	4.58	0.497	1.27	3993	83.59	8.76	1.57	2.02	0.94	0.31	0.44	3.95	0.25
SW3	5	462	4.46	0.562	1.47	3417	140.50	5.58	1.36	1.70	1.39	0.51	0.57	2.25	0.44
SW4	5	336	4.35	0.470	1.23	4030	250.16	5.43	1.62	1.84	0.76	0.64	0.54	1.32	0.76
SW5	4	260	7.18	0.584	1.26	2757	124.25	4.30	1.59	1.69	1.49	0.41	0.74	2.16	0.46
SW6	5	737	4.90	0.519	1.32	3038	84.32	6.67	1.51	1.69	2.05	0.51	0.47	2.40	0.42
SW7	4	123	4.66	0.511	1.42	3028	218.47	3.07	1.41	1.61	0.65	0.58	0.88	1.49	0.67
SW8	5	231	3.70	0.518	1.61	2937	205.24	4.31	1.24	1.57	1.29	0.62	0.64	1.51	0.66
SW9	4	102	4.46	0.651	1.41	2255	151.55	2.75	1.42	1.60	1.12	0.46	0.40	2.34	0.43
SW10	5	307	4.77	0.531	1.35	2024	91.09	4.27	1.48	1.60	0.63	0.50	0.67	2.15	0.47
SW11	5	312	4.47	0.488	1.38	2017	166.97	5.63	1.45	2.00	1.15	0.65	0.49	1.31	0.76
SW12	5	182	3.68	0.522	1.20	1702	102.10	3.70	1.66	1.73	0.59	0.56	0.79	2.05	0.49
SW13	6	365	3.51	0.539	1.44	2051	102.91	5.14	1.39	1.78	0.99	0.49	0.43	2.11	0.47
SW14	4	33	2.82	0.769	1.14	775	154.08	1.62	1.76	2.07	0.46	0.34	0.64	1.09	0.92
SW15	4	69	4.20	0.601	1.39	1902	180.63	2.51	1.44	1.83	1.14	0.43	0.68	2.67	0.37
SW16	5	98	3.04	0.841	1.20	1150	98.21	2.36	1.67	1.77	0.60	0.35	0.90	1.13	0.89
SW17	5	472	4.38	0.465	1.20	2120	78.25	5.88	1.66	1.72	1.47	0.49	0.51	1.80	0.55
Average	4.8	482.1	4.34	0.610				1.33	4.96	1.52	1.05	0.45	0.59	2.05	0.55

U: Stream Order No.	Nu: Total Stream No.	Rb: Bifurcation Ratio	Rl: Stream Length Ratio
Lg: Length of Overland Flow	Bh: Basin Relief	Rr: Relief Ratio	Dt: Drainage Texture
Dd: Drainage Density	Fs: Stream Frequency	Cc: Compactness Coefficient	Rc: Circulatory Ratio
Re: Elongation Ratio	Bs: Shape Factor	Rf: Farm Factor	

The CF approach was used to rank SWs according to their vulnerability to erosion. This technique is based on knowledge-driven modeling (Todorovski and Dzeroski, 2006). This approach translates a qualitative understanding of a phenomenon based on scientific knowledge into a quantitative assessment that gives equal weight to all criteria, thus it can only be used for comparative assessment. This method has been widely utilized to quantify erosion risk at the watershed level (Panday et al., 2009; Javed et al., 2009; Londhe et al., 2010; Chen et al., 2011; McCloskey et al., 2011; Mosbahi et al., 2012, Jang et al., 2013; Altaf et al., 2014; Farhan and Anaba, 2016; Balasubramanian et al., 2017; Singh and Singh, 2018; Bhattacharya et al., 2019; Nitheshnirmal et al., 2019; Hembram and Shah, 2020).In the CF approach, the value of the CF depends on the total number of SWs (Altaf et al., 2014). Because the Swat River watershed has 17 SWs, they were assigned a rank of 1 to 17 for each of the assessed parameters. For the Group 1 parameters, the SW with the highest value was ranked at 1, while the SW with the lowest value was ranked 17th. In contrast, for the Group 2 parameters, the SW with the lowest value was ranked first and that with the highest was ranked 17th. Table 4 summarizes the rankings of the SWs according to each of the geomorphometric parameters.After ranking the SWs for all of the specified parameters, the rankings for a given SW were added and divided by the total number of parameters to obtain its average rank, which is referred to as the CF. The CF represents the combined influence of all parameters in a specific SW on the erosion susceptibility of that SW. Equation 1 was used to determine the CF (Altaf et al., 2014; Das, 2014; Patel et al., 2012; Balasubramanian et al., 2017):

$Cp = \frac{1}{n}\sum_{i=0}^{n} R$ where C*p* is the CF of an SW, *Ri* is the rank of that SW for a geomorphometric parameter, and *n* is the number of geomorphometric parameters

Table 4: Ranking of individual SWs based on selected linear, aerial, and relief morphometric parameters and calculation of the compound factor (CF).

SWs	Linear Parameters			Relief Parameters			Aerial Parameters								Tot.	CF	Erosion Susceptibility
	Nu	Rb	Lu	Lg	Bh	Rr	Dt	Dd	Fs	Cc	Rc	Re	Bs	Rf			
	GROUP 1									GROUP 2							
SW1	17	12	17	8	15	1	17	10	16	8	13	17	2	8	145	12.08	Low
SW2	16	13	16	7	16	3	16	11	15	11	16	14	1	11	147	12.25	Low
SW3	13	9	13	16	14	10	12	2	7	5	6	9	6	5	103	8.58	High
SW4	11	7	12	5	10	9	11	13	13	12	2	10	14	12	122	10.17	Moderate
SW5	8	17	9	6	17	17	8	12	5	3	12	4	7	3	94	7.83	High
SW6	15	16	15	9	13	4	15	9	6	2	6	13	4	2	112	9.33	Moderate
SW7	5	14	5	14	12	16	5	4	4	13	4	2	13	13	96	8.00	High
SW8	7	5	7	17	11	15	9	1	1	6	3	7	12	6	81	6.75	V. High
SW9	4	10	3	13	9	11	4	5	2	9	10	16	5	9	90	7.50	High
SW10	9	15	10	10	6	5	7	8	3	14	7	6	8	14	111	9.25	Moderate
SW11	10	11	8	11	5	13	13	7	14	7	1	12	15	7	116	9.67	Moderate
SW12	6	4	6	2	3	7	6	14	9	16	5	3	10	16	97	8.08	High
SW13	12	3	11	15	7	8	10	3	11	10	8	15	9	10	117	9.75	Moderate
SW14	1	1	1	1	1	12	1	17	17	17	15	8	17	17	113	9.42	Moderate
SW15	2	6	2	12	4	14	3	6	12	8	11	5	3	8	78	6.50	V. High
SW16	3	2	4	3	2	6	2	16	10	15	14	1	16	15	101	8.42	High
SW17	14	8	14	4	8	2	14	15	8	4	9	11	11	4	116	9.67	Moderate

U: Stream Order No.	Nu: Total Stream No.	Rb: Bifurcation Ratio	Rl: Stream Length Ratio
Lg: Length of Overland Flow	Bh: Basin Relief	Rr: Relief Ratio	Dt: Drainage Texture
Dd: Drainage Density	Fs: Stream Frequency	Cc: Compactness Coefficient	Rc: Circulatory Ratio
Re: Elongation Ratio	Bs: Shape Factor	Rf: Farm Factor	

4. Results And Discussion

4.1. Linear parameters

4.1.1 Stream order (U)

Several stream ordering methods have been employed to characterize and study drainage basins, including those proposed by Horton (1945), Strahler (1964), Shreve (1966), and Hodgkinson et al. (2006). However, because of its simplicity, the Strahler stream order system was adopted in the present study. In this system, the smallest unbranched tributary is classified as a first-order stream. When two first-order streams meet, they form a second-order stream. The trunk stream, which is supplied by multiple-order streams, is a basin's highest-order stream. Based on this classification, it was found that SW1 and SW2 contained sixth-order streams, while the Swat River was a seventh-order stream. The streams in all of the SWs were arranged in a dendritic pattern, which is indicative of textural homogeneity and no morphological control. The number of streams in each order is presented in Table 3 and Fig. 3A.

4.1.2 Stream number (Nu)

The total number of stream segments from each stream order is referred to as the stream number (Nu). Table 3 and Fig. 3B present the number of streams in Swat River SWs. The analysis revealed that WS1 and WS2 had the highest number of streams, with 2511 and 1597, respectively. In general, the number of streams decreases as the stream order increases within

a watershed. The number of streams in a watershed indicates its permeability and capacity for infiltration. A higher number of streams suggests that the watershed's soil and lithology are less permeable, resulting in greater runoff.

4.1.3 Bifurcation ratio (Rb)

The bifurcation ratio (Rb) is a dimensionless number that represents the ratio of streams in a lower order to the number of streams in the next higher order (Schumn, 1956). The distribution of the mean bifurcation ratio for the Swat River SWs is displayed in Table 3 and Fig. 3C. The analysis revealed that SW5 had a mean bifurcation ratio of 7.18, while SW14 had the lowest ratio (Rb=2.82). A high bifurcation ratio indicates that the SW is under strong structural control, whereas a low ratio suggests that the SW is subject to fewer structural disruptions (Hembram and Saha, 2008). The difference in the bifurcation ratio between SWs is determined by the watershed's lithology, soil properties, and configuration (Strahler, 1957). For example, in comparison to circular basins, elongated watersheds have a higher ratio (Ali et al., 2018). Suresh (2007) argued that a bifurcation ratio of 3–5 suggests that surface geology has little influence on the drainage pattern. Elongated basins with a higher bifurcation ratio exhibit a low but prolonged flow, whereas circular basins with a low bifurcation ratio experience sudden peaks in water flow (Harinath and Raghu, 2013).

4.1.4 Stream length ratio (R_L)

As defined by Horton (1945), the stream length ratio is the geometrical relationship between the mean stream length and the stream order. In general, as the stream order increases, the stream length decreases. Changes in the stream length ratio are related to variation in the slope and topography of an SW (Waikar and Nilawar, 2014), and this has a substantial impact on runoff and soil erosion (Horton, 1945). Table 3 and Fig. 3D present the regional distribution of the stream length ratio for the Swat River SWs which ranged from 0.465 for SW17 to 1.271 for SW1.

4.2. Aerial parameters

4.2.1 Drainage density (D_d)

The drainage density (D_d) is the ratio of the length of all stream segments within a drainage basin to the drainage area, and it thus represents the relationship between form attributes and geomorphic processes in action (Welling, 1973). It is indicative of land usage and infiltration and the reaction time between rainfall and outflow. A high drainage density indicates high runoff and thus high soil erosion (Roger, 1980). It also indicates the erosive potential of runoff and the erodibility of the surface, and it is a measure of the drainage efficiency of watershed streams. Geology/lithology and plant cover influence the drainage density. Sedimentary rocks with high permeability minimize surface runoff and, as a result, have a low drainage density. In contrast, a high drainage density reflects a low plant density and the limited infiltration capability of the watershed. The drainage density of the SWs ranged from 1.62 for SW14 to 12.41 for SW1, with an average of 4.96 (Table 3 and Fig. 4A).

4.2.2 Drainage frequency (Fs)

According to Horton (1945), the drainage frequency is the number of stream segments per unit area. It is a key measure for understanding the erosion risk of watersheds. The drainage frequency represents the degree of the dissection of the basin and is largely determined by the basin's lithology, plant cover, soil infiltration capacity, catchment relief, drainage network texture, and precipitation (Parveen et al. 2012). It is derived by dividing the total number of streams by the drainage basin area. The average drainage frequency in the research region was found to be 1.52. The maximum drainage frequency was 2.07 for SW14, while the lowest was 1.57 for SW8 (Table 3 and Fig. 4B).

4.2.3 Length of overland flow (Lg)

The length of overland flow (Lg) is the distance that water travels over the ground surface before being concentrated within a stream channel. It is calculated as half of the drainage density (Horton, 1945). The length of overland flow is inversely related to the average channel slope and is considered to be one of the most significant characteristics determining both the hydrologic and hydrographic development of drainage basins (Horton, 1945; Patel et al., 2012; Mokarram and Sathyamoorthy, 2015; Farhan and Anaba, 2016). The average length of overland flow for the SWs ranged from 1.20 to 1.61 for SW17 and SW8, respectively (Table 3 and Fig. 4C.)

4.2.4 Drainage texture (D_t)

The drainage texture (D_t) is the ratio between the total number of streams of all orders and the perimeter of the drainage basin (Horton, 1945). This ratio represents the relative spacing of streams. Smith (1950) categorized drainage texture as extremely coarse (>2), coarse (2–4), moderate (4–6), fine (6–8), and very fine (>8), with a higher drainage texture generally indicating a higher sensitivity to erosion. The drainage texture is determined by the precipitation, vegetation, geology, soil type, soil permeability, and basin relief. The drainage texture for the study area was 1.33, representing a highly coarse texture. However, it ranged from 1.62 to 12.41 for SW14 and SW1, respectively, representing a very fine to a very coarse textural range (Table 3 and Fig. 4D).

4.2.5 Compactness coefficient (Cc)

According to Gravelius (1914), the compactness coefficient of a watershed is the ratio of the watershed perimeter to the circumference of the circle encompassing the watershed area. It is also known as the Gravelius index (GI). The compactness coefficient is independent of the size of the watershed; rather, it is determined by its slope (Horton, 1945). Circular watersheds have a shorter period of concentration before peak runoff, hence a compactness coefficient of less than 1.0 indicates greater divergence from a circular shape (Altaf et al., 2013). A higher compactness coefficient indicates a circular watershed and greater erosion, whereas a lower compactness coefficient indicates the elongation of the watershed and hence reduced susceptibility to erosion (Farhan and Anaba, 2016). The average compactness coefficient of the Swat River basin was 1.05, indicating increased erosion; however, it varies from 2.05 to 0.60 for SW6 and SW16, respectively (Table 3 and Fig. 5A).

4.2.6 Circulatory ratio (R_C)

The circulatory ratio (R_C) is the ratio of the area of the drainage basin (Au) to the area of a circle (Ac) with the same perimeter as the drainage basin (Miller, 1953). The length and frequency of the stream, lithology, land use/land cover, watershed relief, slope, and climatic conditions of the watershed all influence the circulatory ratio (Farhan and Anaba, 2016). Watersheds with a circulatory ratio of 0.4 to 0.5 are considerably elongated (Miller, 1953). A low, moderate, and high circulatory ratio indicates the younger, mature, and older stages of the geomorphic cycle of a watershed, respectively (Magesh et al., 2011). The lower the circulatory ratio, the greater the infiltration and slower the discharge, lowering the risk of erosion. The average circulatory ratio computed for the study area was 0.45, suggesting that the basin is characterized by moderate to low relief and that the drainage pattern is less affected by its structure. It also suggests that the stream frequency and drainage density have a minimal impact on the extent to which the basin surface is affected by degradation processes. A value for the coefficient close to 1 reflects the fan-shaped basin's proclivity for high peak discharge (Parveen et al., 2012). SW4 had the highest circulatory ratio (0.64), while SW2 had the lowest (0.31; Table 3 and Fig. 5B).

4.2.7 Elongation ratio (R_e)

According to Schumm (1956), the elongation ratio is the ratio between the diameter of a circle with the same area as the basin and the maximum length of the basin (L_{max}). The elongation ratio varies from 0.6 to 1.0 depending on the geological units and climate, with <0.7 classified as elongated, 0.8–0.9 as oval, and >0.9 as circular (Waikar and Nilawar, 2014). The average elongation of the study area was 0.59, suggesting an elongated basin and steep slopes (Table 3 and Fig. 5C). The

highest elongation ratio (0.90) was calculated for SW16, while the lowest (0.31) was calculated for SW1. Elongation ratios ranging from 0.6 to 0.8 are generally associated with steep slopes, high relief, and a high rate of erosion (Strahler, 1964).

4.2.8 Shape factor (B_s)

The shape factor, which reflects the shape of the basin, can be calculated by dividing the square of the maximum length of the basin by its total area (Horton, 1945). The shape of the drainage basin, along with its length and ratio, affects the rate of sediment generation and water accumulation. The average shape factor for the Swat River basin was 1.93, indicating a somewhat elongated shape, but it varied from 0.93 to 3.95 for SW11 and SW2, respectively, suggesting that an elongated shape is most common among the SWs, leading to a longer basin lag time (Table 3 and Fig. 5D).

4.2.9 Form factor (R_f)

The form factor is the ratio of the drainage area to the square of the drainage basin length (Horton, 1945). The form factor is often used as an empirical measure of the basin shape. According to Harinath and Raghu (2013), if the form factor is lower than 0.5, the basin may have a flatter flow for a longer duration, while if it is higher than 0.5, the basin has higher peaks for a shorter duration. For a perfectly circular basin, the form factor will always be greater than 0.78; a value smaller than this is indicative of an elongated basin. The average form factor for the Swat River basin was 0.55, suggesting a semicircular shape. The highest form factor was found for SW14 and lowest for SW2 (0.92 and 0.25, respectively; Table 3 and Fig. 6A).

4.3. Relief characteristics

4.3.1 Basin relief (B_h)

The basin relief, which is also known as total relief, is the difference between the elevation of the highest and lowest point on the drainage basin (Schumm, 1956). Basin relief is indicative of the potential energy of a drainage system and is an important factor in understanding the degradational /erosional processes in the catchment area. The higher Bh value indicates a high potential erosional energy, especially during intense rainstorms and flooding. The calculated Bh value Swat River SWs is ranging from 775m to 4030m (Table 3 and Fig. 5B).

4.3.2 Relief ratio (Rr)

The relief ratio is defined as the ratio between the basin relief (Bh) and the maximum basin length (Lb). Schumm, (1956) reported a close relationship between the relief ratio and sediment loss per unit area. The relief ratio of the Swat River SWs ranged from 0.25 to 0.92 (Table 3 and Fig. 5C).

5. Soil Erosion Susceptibility Analysis

In the present study, the soil erosion risk was assessed using the morphometry-based CF approach, which is effective for the evaluation of land-surface processes between similar entities such as watersheds (Ameri et al., 2018). The CFs for each of the 17 SWs were computed by summing the rank values for all 15 linear, aerial, and relief parameters selected for the study and dividing the total by the total number of parameters. The results of the analysis are shown in Table 4 and Fig. 7. The CF ranged from 8.0 to 13.83; the SW with the lowest CF had the highest susceptibility to erosion, while that with the highest CF had the lowest susceptibility. The SWs were subsequently divided into four groups based on the CFs: those with a CF of 8.00–9.00 were classified as having a very high susceptibility, 9.01–10.49 as having a high susceptibility, 10.50–11.49 as having a moderate susceptibility, and 11.50–13.83 as having a low susceptibility to erosion. Fig. 8 presents the classification of the Swat River SWs according to the CF. Overall, three of the SWs (SW8, SW12, and SW15; 18% of the total)

were in the very high-susceptibility group (8.0, 8.9, and 8.9, respectively), while SW1, SW2, and SW4 were in the low-susceptibility group (13.4, 13.8, and 11.8, respectively).

The very high priority SWs had high to moderate values for Group 1 linear and relief morphometric parameters, including the presence of fifth-order streams, an overland flow length of 1.20–1.61, a very high basin relief of 1720–2937, a relief ratio of 102.10–205.24, a shape factor of 1.51–2.67, and a farm factor of 0.37–0.66. These SWs are characterized by loamy soil, with dry farming and grazing taking place on the lower slopes and pines covering the higher slopes. The geology ranges from amphibolite to greenschist and basalt.

6. Validation Of The Results

To validate the results of the present study, they were compared with the soil, land use/land cover, geology, slope, and gradient map of the study area (Fig. 9). It was found that the SWs identified as very highly vulnerable to soil erosion have loamy soil where dry farming is undertaken. Agriculture accounted for 23.72% of the land area of the very highly susceptible SWs, compared to 23.02%, 21.76%, and 17.76% of the SWs with high, moderate, and low susceptibility (Fig. 10). According to Phinizi and Ngetar (2019), soil loss in the forested area decreased from 1989 to 2001 from 0.033 to 0.032 tons/ha^{-1}year^{-1}. In contrast, on agricultural land, the soil loss increased from 0.339 tons/ha^{-1}year^{-1} to 0.376 tons/ha^{-1}year^{-1} from 1989 to 2017. In terms of the geology, the majority of the study area contains igneous and metamorphic rocks, including amphibolite, greenschist, granite, and basalt. A small area in the south contains quaternary alluvium deposits.

The slope and gradient of the SWs appeared to be an important factor in determining the vulnerability of the SWs to soil erosion. Fig. 11 summarizes the slope distribution for each of the erosion-susceptibility classes. It was found that almost 60% of the area of the very highly susceptible SWs had a slope of 29.50–47.12°, compared to only 29.12%, 31.73%, and 44.38% in the high-, moderate-, and low-susceptibility SWs. Similar results were obtained from the gradient analysis (Fig. 9E), with the gradient of very highly susceptible SWs the highest at 180.7–250.2 m/km. The slope has a strong influence on soil erosion (Rather et al., 2017; Balasubramanian et al., 2017), which is why, even though 40.12% of the land area of the SWs with a very high erosion risk had forest cover, their steep gradient still increased their susceptibility. According to Zingg (1940), the volume of soil erosion increases with an increase in the slope gradient, which was later supported by Tang and Chen (1997). Renner (1936) also reported that the percentage of the eroded area varies with the slope gradient, with a critical slope gradient of 40.5°. This is similar to Liu et al. (2001), who found that the critical slope gradient for optimal soil erosion was between 41.5° and 50°, while Horton (1945), Chen (1985), and When-hong (1993) reported it to be 57°, 25°, and 41°, respectively. It has been argued that the slope is an important factor that influences the generation of overland flow and soil erosion (Liu et al., 2001). The stress of overland flow, the erosion-resistance capacity of the soil, and the lithology and overland flow velocity are the main factors that determine the degree of soil erosion on a sloped surface. However, the slope gradient, rainfall intensity, infiltration capacity of the soil, soil structure, LULC, and length of overland flow also affect the rate of soil erosion. Soil erosion resistance decreases with an increase in the slope gradient (Liu et al., 2001).

Overall, the analysis of the soil, geology, land use, slope gradient, and field observations were in agreement with the results derived from the CF approach for the determination of erosion susceptibility. This suggests that the adopted methodology for the prioritization of SWs for erosion management produces reasonable results.

Conclusion

The present study demonstrated that a DEM together with GIS is an efficient tool for the delineation of a drainage network at the SW level and analysis of the associated geomorphometric parameters. The geomorphometry of various linear, aerial, and relief parameters for soil erosion susceptibility in the geospatial environment was found to be suitable for the prioritization of SWs in terms of soil erosion management.

The assessment of the soil erosion susceptibility of Swat River SWs using the morphometry-based CF approach in the geospatial environment revealed that three SWs (SW8, SW12, and SW15; 18% of the total) were prioritized as very highly susceptible to soil erosion, while SW7, SW9, SW10, and SW16 were classified as highly susceptible (23% of the total). A total of 7 SWs (SW3, SW5, SW6, SW11, SW13, SW14, and SW17) were categorized as moderately susceptible (41% of the total), while SW1, SW2, and SW4 had a low susceptibility (18% of the total). The present study revealed that the major morphometric parameters that influence soil erosion were the basin shape and relief parameters, including the basin relief and relief ratio.

Soil erosion is influenced by a range of environmental factors such as the temporal and spatial distribution of rainfall, its intensity and size of the raindrops, the amount and frequency of rain, runoff volume, and velocity. However, it is clear that watershed characteristics such as the slope gradient, aspect, shape, and length of the channel area have a significant impact on the rate of soil erosion. The CF approach used in the present study is one of the most widely used approaches for erosion susceptibility at the SW level. It is simple to employ but has some inherent disadvantages, particularly that it is only applicable to comparative studies. However, the prioritization of SWs using the CF approach remains useful for planners and decision-makers in terms of devising soil conservation strategies.

References

1. Ali U, Ali SA, Ikbal J, Bashir M, Fadhi M., Ahmad M, ... Ali S (2018) Soil erosion risk and flood behavior assessment of Sukhang catchment, Kashmir basin: Using GIS and remote sensing. J Remote Sens GIS, 7(1): 1-8.
2. Altaf F, Meraj G, Romshoo SA (2013) Morphometric analysis to infer hydrological behaviour of Lidder watershed, Western Himalaya, India. Geog J
3. Altaf, S, Meraj, G, Romshoo SA (2014) Morphometry and land cover based multi-criteria analysis for assessing the soil erosion susceptibility of the western Himalayan watershed. Environ Monit Assess 186(12): 8391-8412.
4. Ameri AA, Pourghasemi HR, Cerda A (2018) Erodibility prioritization of sub-watersheds using morphometric parameters analysis and its mapping: A comparison among TOPSIS, VIKOR, SAW, and CF multi-criteria decision making models. Sci Tot Environ 613: 1385-1400.
5. Amiri M, Pourghasemi HR (2020) Mapping and Preparing a Susceptibility Map of Gully Erosion Using the MARS Model. In Gully Erosion Studies from India and Surrounding Regions (pp. 405-413). Springer, Cham.
6. Arabameri A, Chen W, Lombardo L, Blaschke T, Tien Bui D (2020) Hybrid computational intelligence models for improvement gully erosion assessment. Remote Sens 12(1): 140.
7. Arshad MA, Martin S (2002) Identifying critical limits for soil quality indicators in agro-ecosystems. Agric Ecosyst Environ 88(2): 153-160.
8. Avand M, Janizadeh S, Naghibi SA, Pourghasemi HR, Khosrobeigi Bozchaloei S, Blaschke T (2019) A comparative assessment of Random Forest and k-Nearest Neighbor classifiers for gully erosion susceptibility mapping. Water 11(10): 2076.
9. Azareh A, Rafiei Sardooi E, Choubin B, Barkhori S, Shahdadi A, Adamowski J, Shamshirband, S (2019) Incorporating multi-criteria decision-making and fuzzy-value functions for flood susceptibility assessment. Geocarto Int 1-21.
10. Azizian Shokoohi A (2015) Effects of data resolution and stream delineation threshold area on the results of a kinematic wave based GIUH model. Water South Africa 41(1): 61-69.
11. Balasubramanian A, Duraisamy K, Thirumalaisamy S, Krishnaraj S, Yatheendradasan RK (2017) Prioritization of subwatersheds based on quantitative morphometric analysis in lower Bhavani basin, Tamil Nadu, India using DEM and GIS techniques. Arab J Geosci 10(24): 552.
12. Bayramin İ, Dengiz O, Başkan O, Parlak M (2003) Soil erosion risk assessment with ICONA model; case study: Beypazarı area. Turk J Agric For 27(2): 105-116.

13. Berberoglu S, Cilek A, Kirkby M, Irvine B, Donmez C (2020) Spatial and temporal evaluation of soil erosion in Turkey under climate change scenarios using the Pan-European Soil Erosion Risk Assessment (PESERA) model. Environ Monit Assess 192(8): 1-22.
14. Bhattacharya RK, Chatterjee ND, Das K (2019) Multi-criteria-based sub-basin prioritization and its risk assessment of erosion susceptibility in Kansai–Kumari catchment area, India. Appl Water Sci 9(4): 76.
15. Borrelli P, Robinson DA, Fleischer LR, Lugato E, Ballabio C, Alewell C, ... Panagos P (2017) An assessment of the global impact of 21st century land use change on soil erosion. Nat Commun 8(1): 1-13.
16. Brooks ES, Dobre M, Elliot WJ, Wu JQ, Boll J (2016) Watershed-scale evaluation of the Water Erosion Prediction Project (WEPP) model in the Lake Tahoe basin. J Hydrol, 533: 389-402.
17. Buccolini M, Coco L, Cappadonia C, Rotigliano E (2012) Relationships between a new slope morphometric index and calanchi erosion in northern Sicily, Italy. Geomorphology 150: 41–48.
18. Chen L, Qian X, Shi Y (2011) Critical area identification of potential soil loss in a typical watershed of the three Gorges reservoir region. Water Resour Manag 25(13): 3445.
19. Chen W, Li Y, Xue W, Shahabi H, Li S, Hong H, Wang X, Bian H, Zhang S, Pradhan B, et al. 2020. Modeling flood susceptibility using data-driven approaches of naïve Bayes tree, alternating decision tree, and random forest methods. Sci Total Environ. 701: 134979
20. Chen FY (1985) The experiments of the effects of the slope on soil erosion. Chinese Soil Water Conserv 2: 24-30.
21. Chuenchum P, Xu M, Tang W (2020) Estimation of soil erosion and sediment yield in the Lancang–Mekong River using the Modified Revised Universal Soil Loss Equation and GIS techniques. Water, 12(1), 135.
22. Cutter SL, Barne L, Berry M, Burton C, Evans E, Tate E, Webb J (2008) A place-based model for understanding community resilience to natural disasters. Glob Environ Change 18, 598–606
23. Das, D (2014) Identification of erosion prone areas by morphometric analysis using GIS. J Instf Eng 95(1): 61-74.
24. Debelo G, Tadele K, Koriche SA (2017) Morphometric analysis to identify erosion prone areas on the upper blue Nile using GIS (Case study of Didessa and Jema sub-basin, Ethiopia). Int Res J Eng Technol 4(08): 1773-1784.
25. DeMars C, Zhan Y, Chen H, Heilman P, Zhang X, Zhang M (2018) Integrating GLEAMS sedimentation into RZWQM for pesticide sorbed sediment runoff modeling. Environ Model Software, 109: 390-401.
26. Duarte A (2019). Hopper system design using CFD–Warsak HPS Water-intake (Pakistan). Conference Paper: Bend and Straight Open-Channel Experimental Research.
27. Eroğlu H, Çakır G, Sivrikaya F, Akay AE (2010) Using high resolution images and elevation data in classifying erosion risks of bare soil areas in the Hatila Valley Natural Protected Area, Turkey. Stoch Environ Res Risk Assess 24(5): 699-704.
28. Esmaeili Gholzom H, Ahmadi H, Moeini A, Motamed Vaziri B (2020) Erosion risk assessment and identification of susceptibility lands using the ICONA model and RS and GIS techniques. Nat Hazards Earth Syst Sci Discuss 1-18.
29. Farhan Y, Anaba, O (2016) A remote sensing and GIS approach for prioritization of Wadi Shueib Mini-Watersheds (Central Jordan) based on morphometric and soil erosion susceptibility analysis. J Geogr Inf Sys 8(1): 1-19.
30. Gayen A, Saha S (2017) Application of weights-of-evidence (WoE) and evidential belief function (EBF) models for the delineation of soil erosion vulnerable zones: a study on Pathro river basin, Jharkhand, India. Model Earth Sys Environ 3(3): 1123-1139.
31. Ghabbour EA, Davies G, Misiewicz T, Alami RA, Askounis EM, Cuozzo NP, ... Shade J (2017) National comparison of the total and sequestered organic matter contents of conventional and organic farm soils. In Advances in Agronomy (Vol. 146, pp. 1-35). Academic Press.
32. Gudino-Elizondo N, Biggs TW, Castillo C, Bingner RL, Langendoen EJ, Taniguchi KT, ... Liden D (2018) Measuring ephemeral gully erosion rates and topographical thresholds in an urban watershed using unmanned aerial systems and structure from motion photogrammetric techniques. Land Degrad Dev 29(6): 1896-1905.

33. Gravelius H (1914) Grundriß der gesamten Gewasserkunde, Band 1: Flußkunde. Compendium of Hydrology, I. 265-278. (Ground plan of the entire hydrology, Volume 1: Flußkunde. Compendium of Hydrology)
34. Grohmann CH, Riccomini C, Alves FM (2007) STRM-based morphotectonic analysis of the Procos de Caldas Alkaline Massif, Southeastern Brazil. Comput Geosci 33, 10-19. http://dx.doi.org/10.1016/j.cageo.2006.05.002.
35. Harinath V, Raghu V (2013) Morphometric analysis using Arc GIS techniques: a case study of Dharurvagu, south eastern part of Kurnool district, Andhra Pradesh, India. Int J Sci Res 2(1): 2319-7064.
36. Hembram TK, Saha S (2020) Prioritization of sub-watersheds for soil erosion based on morphometric attributes using fuzzy AHP and compound factor in Jainti River basin, Jharkhand, Eastern India. Environ Dev Sustain 22(2): 1241-1268.
37. Hillier S (2001) Particulate composition and origin of suspended sediment in the R. Don, Aberdeenshire, UK. Sci Total Environ 265(1-3): 281-293.
38. Hodgkinson JH, Mcloughlin S, Cox M (2006) The influence of structural grain on drainage in a metamorphic sub-catchment: Laceys Creek, southeast Queensland, Australia. Geomorphology 81, 394-407.
39. Horton HE (1945) Erosional development of streams and their drainage basin: Hydro physical approach to quantitative morphology, Geol Soc Am Bull 56, 275-370.
40. Hosseini FS, Choubin B, Mosavi A, Nabipour N, Shamshirband S, Darab, H, Haghighi AT (2020) Flash-flood hazard assessment using ensembles and Bayesian-based machine learning models: application of the simulated annealing feature selection method. Sci Total Environ 711, 135161.
41. Jang T, Vellidis G, Hyman JB, Brooks E, Kurkalova LA, Bol, J, Cho J (2013) Model for prioritizing best management practice implementation: sediment load reduction. Environ Manag 51(1): 209-224.
42. Javed A, Khanday MY, Ahmed R (2009) Prioritization of sub-watersheds based on morphometric and land use analysis using remote sensing and GIS techniques. J Indian Soc Remote Sens 37(2): 261.
43. Jothimani M, Abebe A, Dawit Z (2020) Mapping of soil erosion-prone sub-watersheds through drainage morphometric analysis and weighted sum approach: a case study of the Kulfo River basin, Rift valley, Arba Minch, Southern Ethiopia. Model Earth Syst Environ 6: 2377-2389.
44. Kacem L, Igmoullen B, Mokhtari S, Amar H, Agoussine M (2014) Morphometric characterization of upstream mountain watershed using geographic information system (GIS): high valley of Tifnoute- High Moroccan Atlas. J Biodivers Environ Sci 5(6): 62-66.
45. Kadam AK, Jaweed TH, Kale SS, Umrikar BN, Sankhua RN (2019) Identification of erosion-prone areas using modified morphometric prioritization method and sediment production rate: a remote sensing and GIS approach. Geomatics Nat Hazards Risk 10(1): 986-1006.
46. Kanth TA, Hassan Z (2012) Morphometric analysis and prioritization of watershed for soil and water resource management in Wular catchment using geo-spatial tools. Int J Geol, Earth Environ Sci 2(1): 30-41
47. Karydas C, Panagos P (2020) Towards an assessment of the ephemeral gully erosion potential in Greece using Google Earth. Water, 12(2), 603.
48. Keesstra SD, Bouma J, Wallinga J, Tittonell P, Smith P, Cerdà A, ... Fresco LO (2016) The significance of soils and soil science towards realization of the United Nations Sustainable Development Goals. Soil, 2: 111-128.
49. Londhe S, Nathawat MS, Subudhi AP (2010) Erosion susceptibility zoning and prioritization of miniwatersheds using geomatics approach. Int J Geomat Geosci 1(3): 511-528.
50. Liu QQ, Chen L, Li JC (2001) Influences of slope gradient on soil erosion. Appl Math Mech 22(5): 510-519.
51. Magesh NS, Chandrasekar N, Soundranayagam JP (2011) Morphometric evaluation of Papanasam and Manimuthar watersheds, parts of Western Ghats, Tirunelveli district, Tamil Nadu, India: a GIS approach. Environ Earth Sci 64(2): 373-381.
52. Martins AK, Giga BL (2015) Hydrological and morphometric analysis of upper Yadzaram Catchment of Mubi in Adamawa State, Nigeria, Using Geographic Information System (GIS). World Environ 5(2): 63-69.

53. Maqsoom A, Aslam B, Hassan U, Kazmi ZA, Sodangi M, Tufail RF, Farooq D (2020) Geospatial assessment of soil erosion intensity and sediment yield using the Revised Universal Soil Loss Equation (RUSLE) model. ISPRS Int J Geo-Inf 9(6): 356.
54. McCloskey JT, Lilieholm RJ, Cronan C (2011) Using Bayesian belief networks to identify potential compatibilities and conflicts between development and landscape conservation. Landsc Urban Plan 101(2): 190-203.
55. Miller VC (1953) Quantitative geomorphic study of drainage basin characteristics in the Clinch Mountain area, Virginia and Tennessee. Technical report (Columbia University. Department of Geology); no. 3.
56. Mohammed S, Alsafadi K, Talukdar S, Kiwan S, Hennawi S, Alshihabi O, ... Harsanyie E (2020) Estimation of soil erosion risk in southern part of Syria by using RUSLE integrating geo informatics approach. Remote Sens Appl: Soc Environ 20: 100375.
57. Mokarram M, Sathyamoorthy D (2015) Morphometric analysis of hydrological behavior of North Fars watershed, Iran. Eur J Geog 6(4), 88-106.
58. Mosavi A, Golshan M, Janizadeh S, Choubin B, Melesse AM, Dineva AA (2020b) Ensemble models of GLM, FDA, MARS, and RF for flood and erosion susceptibility mapping: a priority assessment of sub-basins. Geocarto Int 1-20.
59. Mosavi A, Sajedi-Hosseini F, Choubin B, Taromideh F, Rahi G, Dineva AA (2020a). Susceptibility mapping of soil water erosion using machine learning models. Water, 12(7): 1995.
60. Mundetia N, Sharma D, Dubey SK (2018) Morphometric assessment and sub-watershed prioritization of Khari River basin in semi-arid region of Rajasthan, India. Arab J Geosci 11(18): 530.
61. Murtaza KO, Romshoo SA (2014) Determining the suitability and accuracy of various statistical algorithms for satellite data classification. Int J Geomat Geosci 4(4): 585-599.
62. Nasir MJ, Iqbal J, Ahmad W (2020) Flash flood risk modeling of swat river sub-watershed: a comparative analysis of morphometric ranking approach and El-Shamy approach. Arab J Geosci 13(20): 1-19.
63. Nitheshnirmal S, Thilagaraj P, Rahaman SA, Jegankumar R (2019) Erosion risk assessment through morphometric indices for prioritisation of Arjuna watershed using ALOS-PALSAR DEM. Model Earth Sys Environ 5(3): 907-924.
64. Pandey A, Chowdary VM, Mal BC, Billib M (2009) Application of the WEPP model for prioritization and evaluation of best management practices in an Indian watershed. Hydrol Process: Int J 23(21): 2997-3005.
65. Patel DP, Dholakia MB, Naresh N, Srivastava PK (2012) Water harvesting structure positioning by using geo-visualization concept and prioritization of mini-watersheds through morphometric analysis in the Lower Tapi Basin. J Ind Soc Remote Sens 40(2): 299-312.
66. Parveen R, Kumar U, Singh VK (2012) Geomorphometric characterization of Upper South Koel Basin, Jharkhand: a remote sensing & GIS approach. J Water Resour Prot 4(12): 1042.
67. Pham TG, Degener J, Kappas M (2018) Integrated universal soil loss equation (USLE) and Geographical Information System (GIS) for soil erosion estimation in A Sap basin: Central Vietnam. Int Soil Water Conserv Res 6(2): 99-110.
68. Phinzi K, Ngetar NS (2019) Land use/land cover dynamics and soil erosion in the Umzintlava catchment (T32E), Eastern Cape, South Africa. Trans R Soc South Africa 74(3): 223-237.
69. Pimentel D, Burgess M (2013) Soil erosion threatens food production. Agric 3(3): 443-463.
70. Powlson DS, Gregory PJ, Whalley WR, Quinton JN, Hopkins DW, Whitmore AP, ... Goulding K W (2011) Soil management in relation to sustainable agriculture and ecosystem services. Food Policy 36: S72-S87.
71. Rahaman SA, Ajeez SA, Aruchamy S, Jegankumar R (2015) Prioritization of sub watershed based on morphometric characteristics using fuzzy analytical hierarchy process and Geographical Information System–A study of Kallar Watershed, Tamil Nadu. Aquatic Procedia 4: 1322-1330.
72. Rather MA, Kumar JS, Farooq M, Rashid H (2017) Assessing the influence of watershed characteristics on soil erosion susceptibility of Jhelum basin in Kashmir Himalayas. Arab J Geosci 10(3): 59.
73. Rekolainen S, Posch M (1993) Adapting the CREAMS model for Finnish conditions. Hydrol Res 24(5): 309-322.

74. Rogers WF (1980) A practical model for linear and nonlinear runoff. J Hydrol 46(1-2): 51-78.
75. Renner FG (1936) Conditions influencing erosion on the Boise River watershed (No. 528). US Department of Agriculture.
76. Sadhasivam N, Bhardwaj A, Pourghasemi HR, Kamaraj NP (2020) Morphometric attributes-based soil erosion susceptibility mapping in Dnyanganga watershed of India using individual and ensemble models. Environ Earth Sci 79(14): 1-28.
77. Schumm SA (1956) Evolution of drainage systems and slopes in badlands at Perth Amboy, New Jersey. Geol Soc Am Bull 67(5): 597-646.
78. Shah SA, Shah NA, Ullah S, Alam MM, Badshah H, Ullah S, Mumtaz AS (2016) Documenting the indigenous knowledge on medicinal flora from communities residing near Swat River (Suvastu) and in high mountainous areas in Swat-Pakistan. J Ethnopharmacol 182, 67-79.
79. Shreve RL (1996) Statistical law of stream numbers. J Geog 1966, 74, 17-37.
80. Singh, O., & Singh, J. (2018). Soil erosion susceptibility assessment of the Lower Himachal Himalayan Watershed. J Geol Soc India, 92(2): 157-165.
81. Smith KG (1950) Standards for grading texture of erosional topography. Am J Sci 248, 655-668
82. Strahler AN (1957) Quantitative analysis of watershed geomorphology. Eos, Trans Am Geophys Union 38(6): 913-920.
83. Strahler AN (1964) Quantitative geomorphology of drainage basin and channel network. In: Chow, V.T., Ed., Handbook of Applied Hydrology, McGraw Hills, New York. (1964).
84. Suresh R (2012) Soil and Water Conservation Engineering. Standard Publishers Distributors.
85. Tan G, Shibasaki R (2003) Global estimation of crop productivity and the impacts of global warming by GIS and EPIC integration. Ecol Model 168(3): 357-370.
86. Tang LQ, Chen GX (1997) The dynamic model of water and soil generation in small watershed. J Hydrodynam, Serials A, 12(2): 164-174.
87. Todorovski L, Džeroski S (2006). Integrating knowledge-driven and data-driven approaches to modeling. Ecol Model 194(1-3): 3-13.
88. Tundu C, Tumbare MJ, Onema JMK (2018) Sedimentation and its impacts/effects on river system and reservoir water quality: case study of Mazowe catchment, Zimbabwe. Proc Int Assoc Hydrol Sci 377: 57.
89. Vaezi AR, Abbasi M, Keesstra S, Cerdà A (2017). Assessment of soil particle erodibility and sediment trapping using check dams in small semi-arid catchments. Catena, 157: 227-240.
90. Vidale M, Olivieri LM (2002) Painted rock shelters of the Swat Valley: Further discoveries and new hypotheses. East and West 52(1/4): 173-223.
91. Waikar ML, Nilawar AP (2014) Morphometric analysis of a drainage basin using Geographical Information System: A case study. Int J Multidiscip curr Res 2: 179-198.
92. Walling DE (2011) Human impact on the sediment loads of Asian rivers. Sediment problems and sediment management in Asian River Basins, IAHS Publ, 349: 37-51.
93. Wakode HB, Dutta D, Desai VR, Baier K, Azzam R (2013) Morphometric analysis of the upper catchment of Kosi River using GIS techniques. Arab J Geosci 6(2): 395–408.
94. Walling DE (1973) Drainage Basin Form and Process: A Geomorphological Approach. Edward Arnold.
95. Wen-hong CAO (1993) On the study of the critical slope of soil erosion. Soil Water Conserv Bull 13(4): 1-5.
96. Zingg AW (1940) Degree and length of land slope as it affects soil loss in run-off. Agric Eng 21: 59-64.

Figures

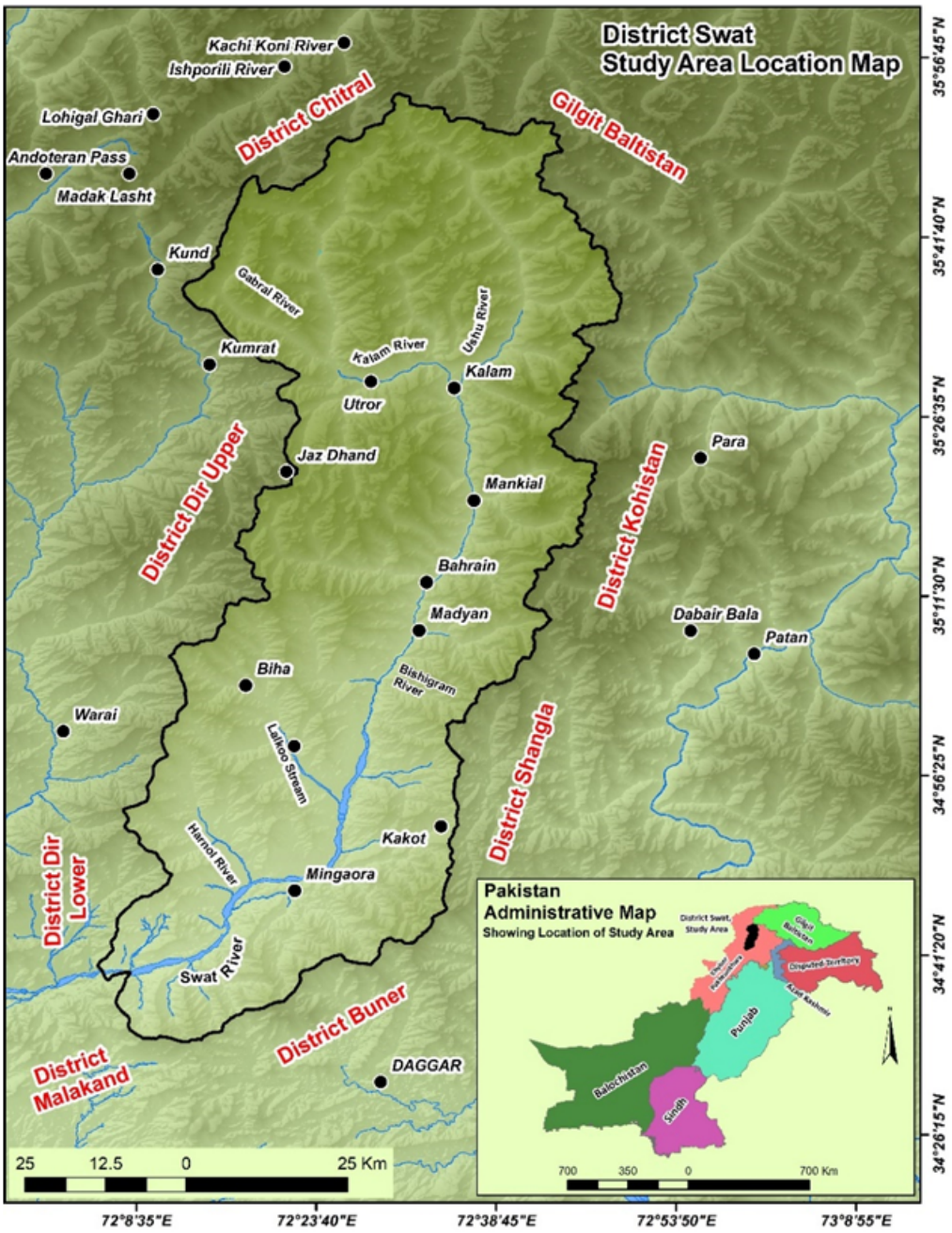

Figure 1

Location of the Swat district, Khyber Pakhtunkhwa, Pakistan

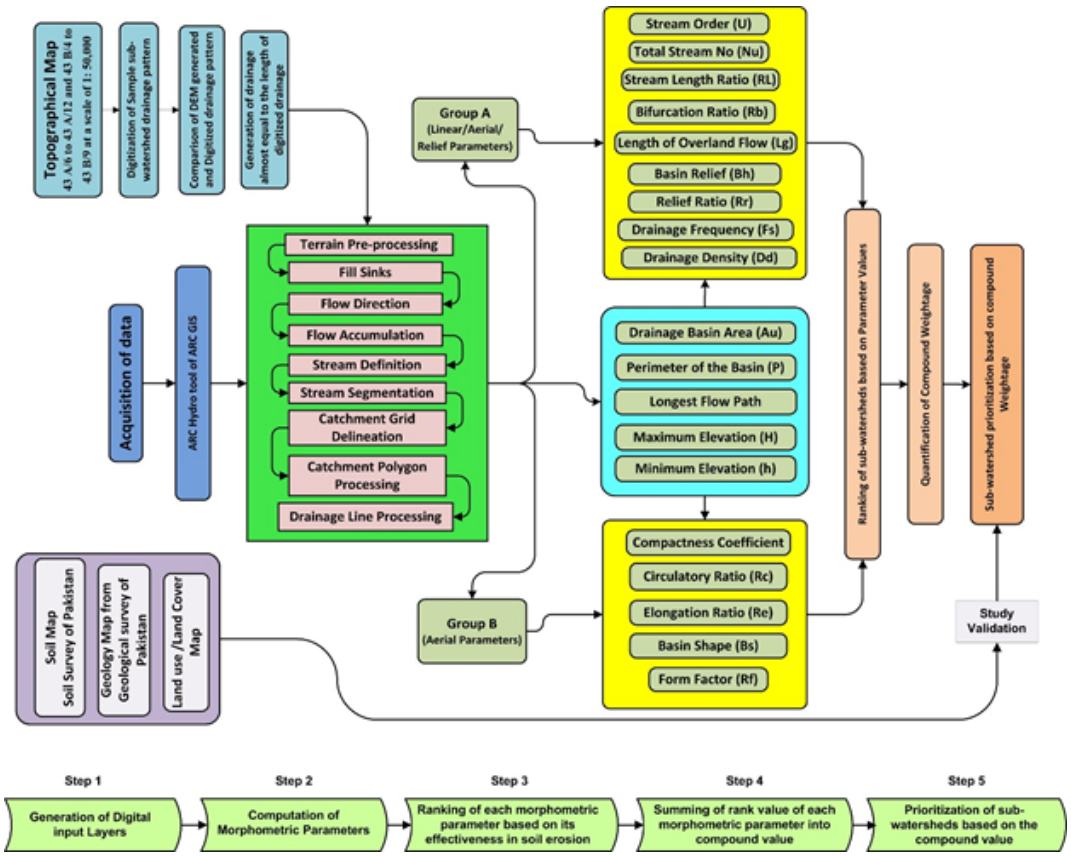

Figure 2

Research methodology adopted from Hembram and Shah (2020).

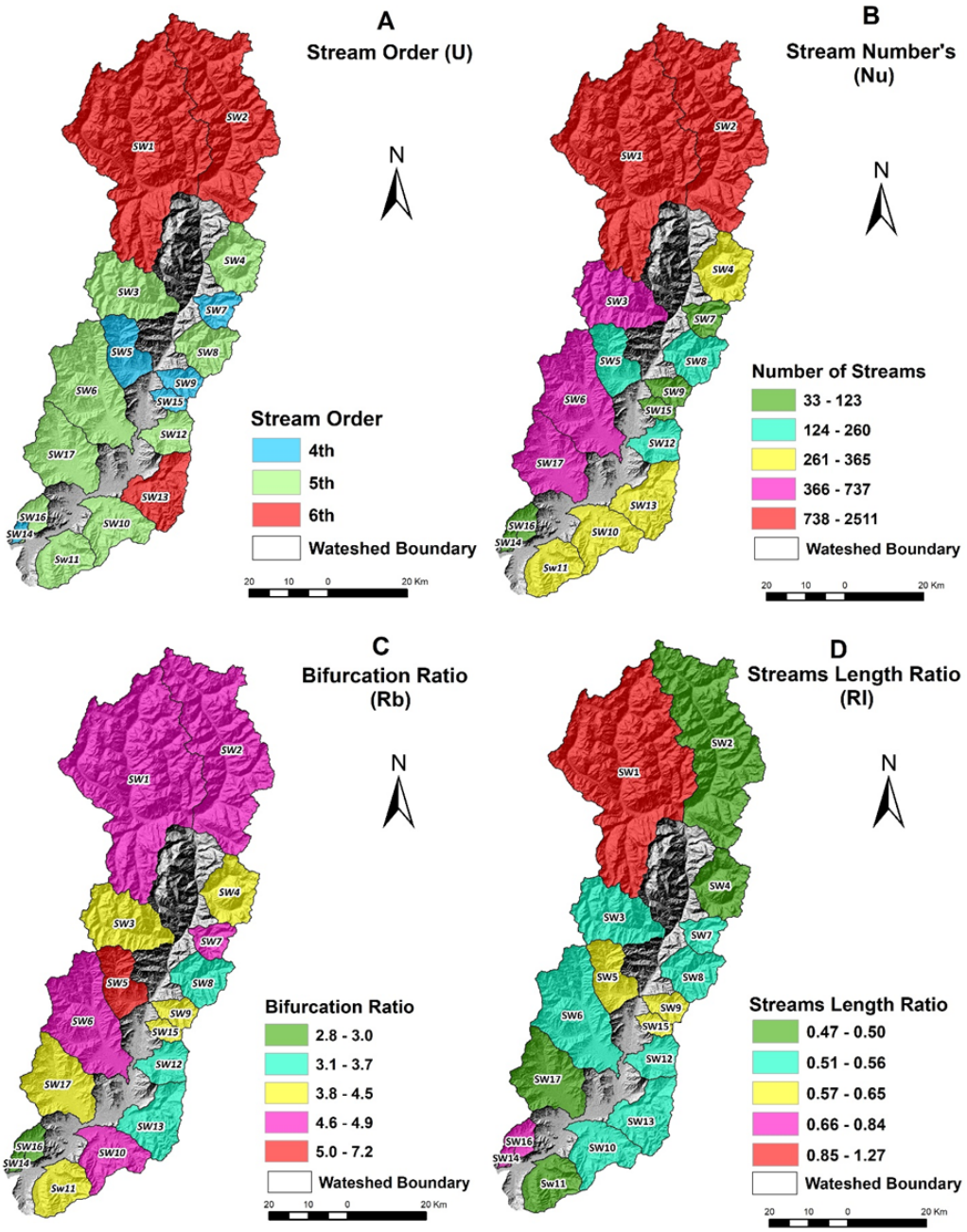

Figure 3

Linear morphometric attributes of the Swat River SWs: **A** stream order, **B** number of streams, **C** bifurcation ratio, and **D** stream length ratio

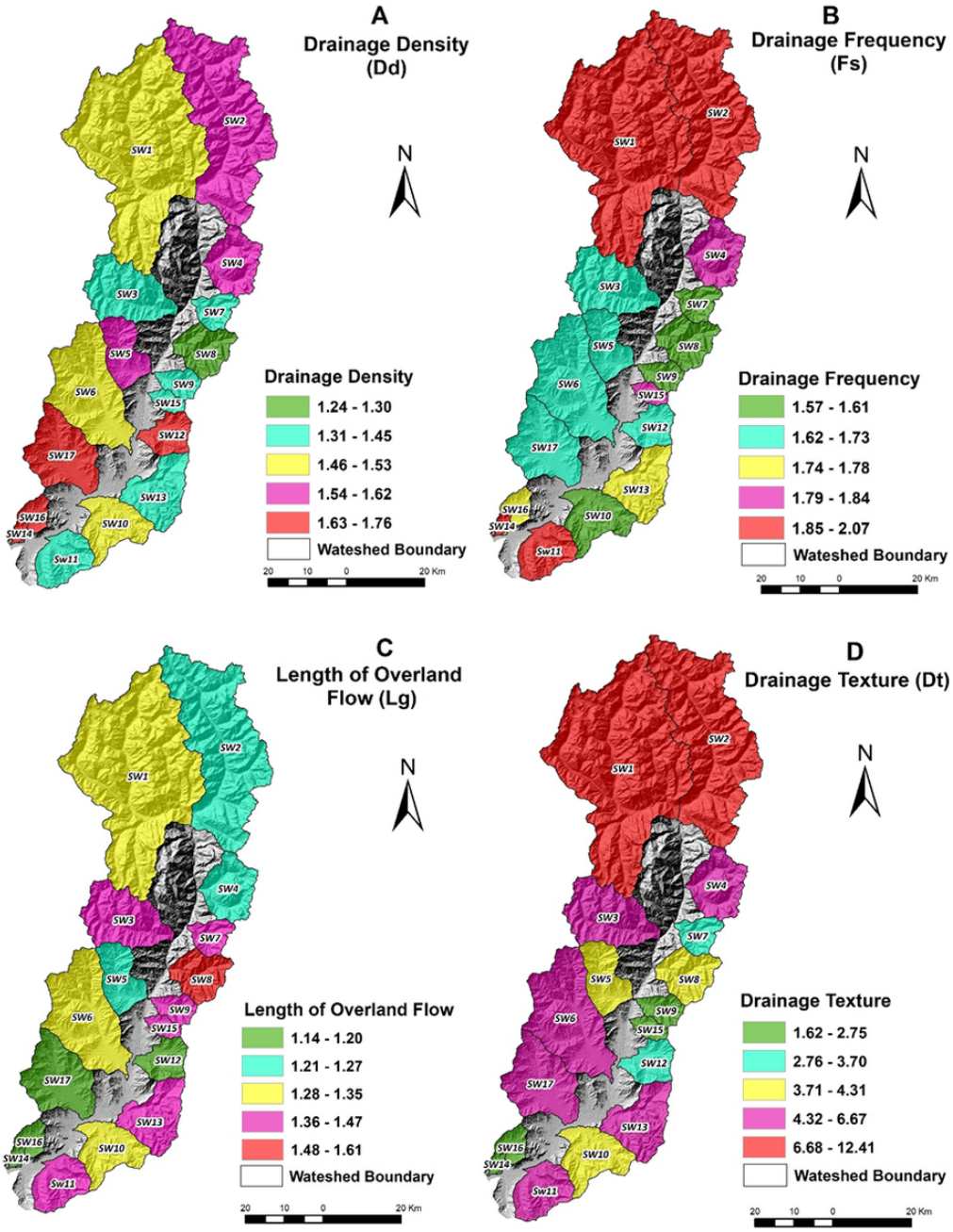

Figure 4

Linear and aerial morphometric attributes of the Swat River SWs: **A** drainage density, **B**drainage frequency, **C** length of overland flow, and **D** drainage texture

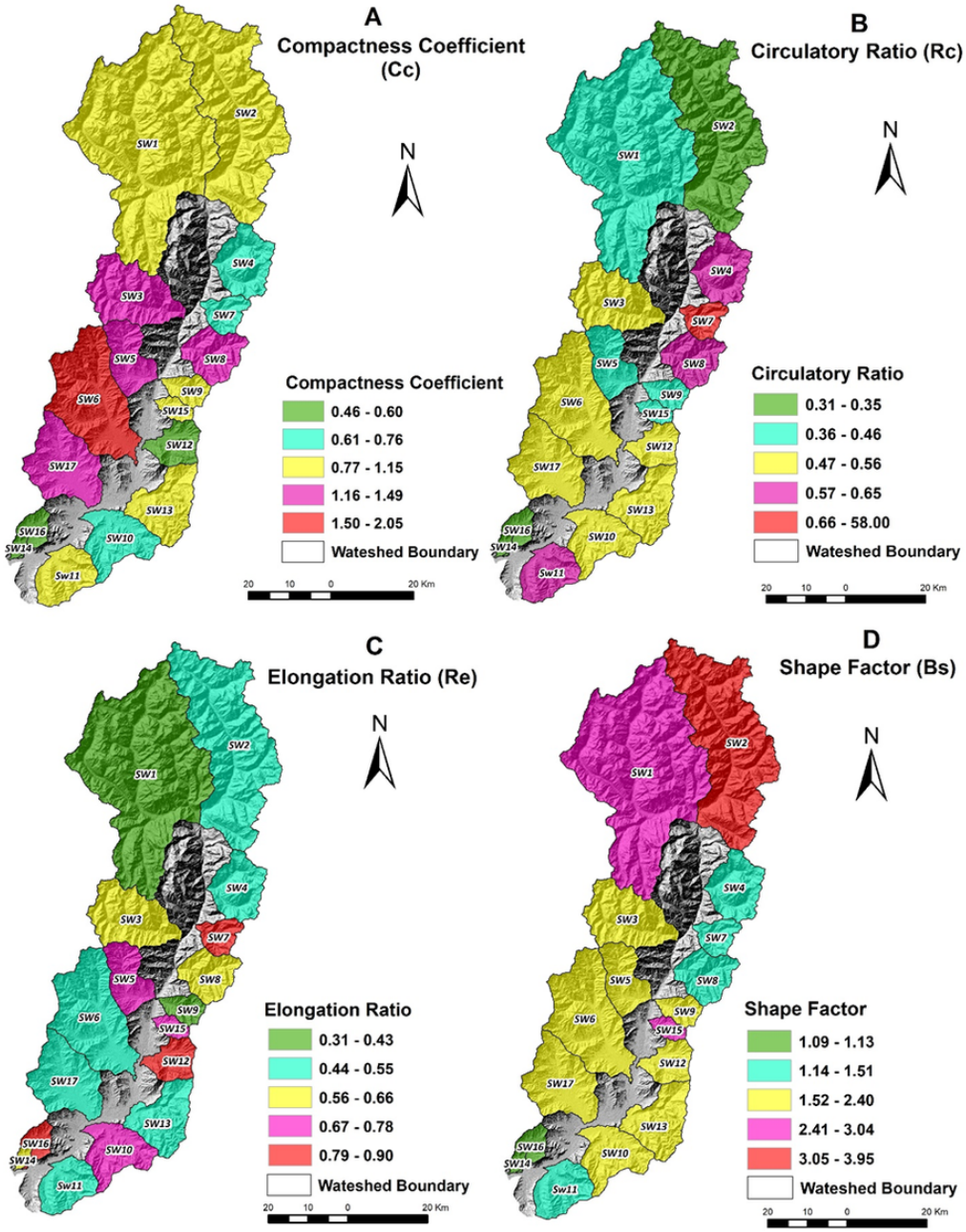

Figure 5

Aerial morphometric attributes of the Swat River SWs: **A** compactness coefficient, **B**circulatory ratio, **C** elongation ratio, and **D** shape factor

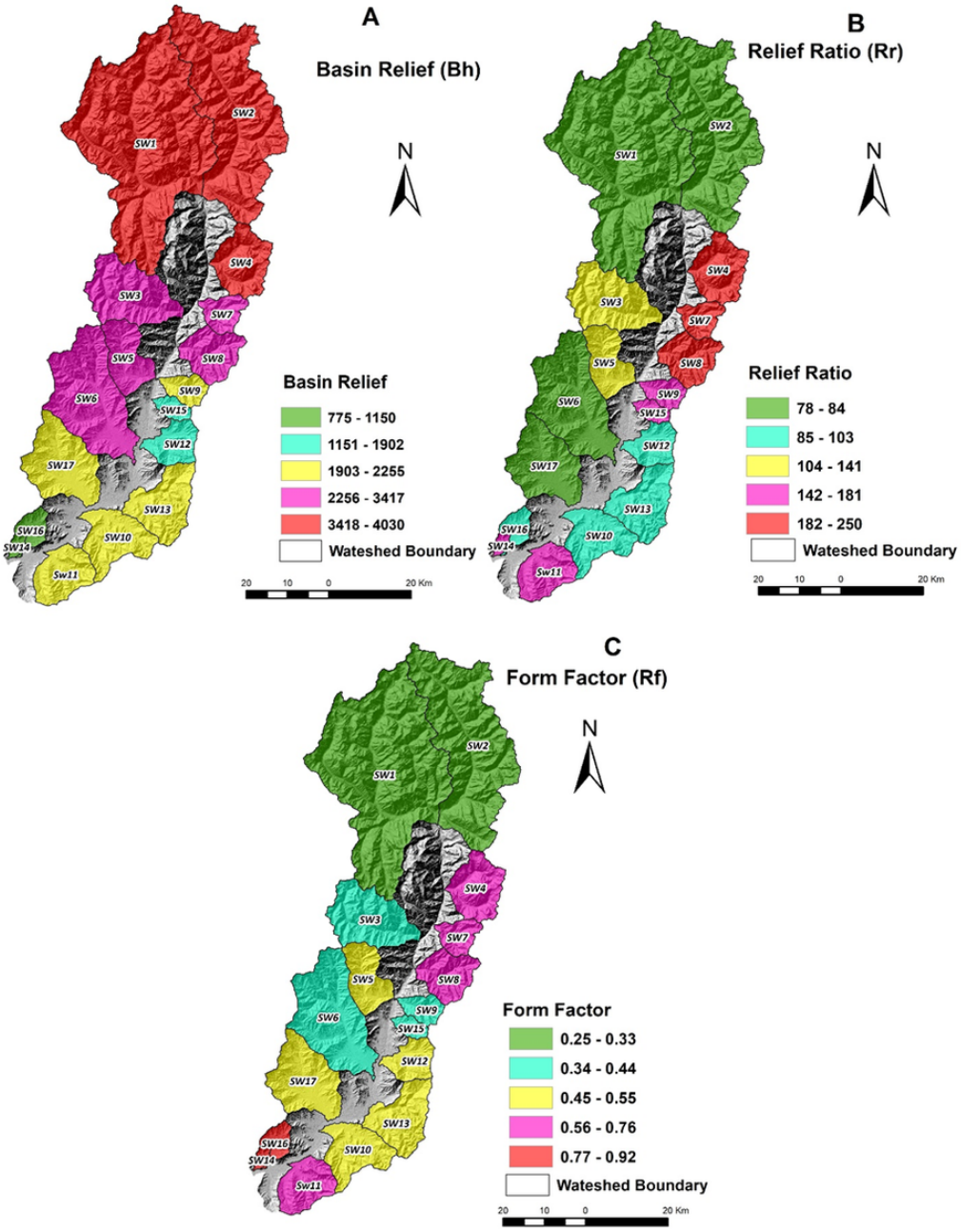

Figure 6

Relief morphometric attributes of the Swat River SWs: **A** basin relief, **B** relief ratio, and **C** form factor

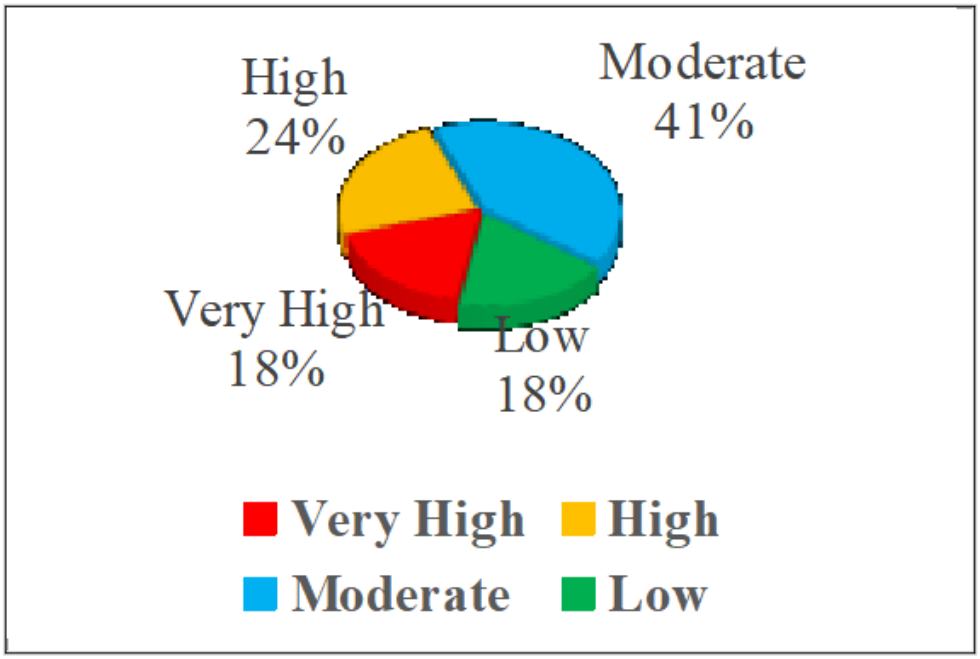

Figure 7

Classification of the Swat River SWs based on their erosion susceptibility determined using the CF approach.

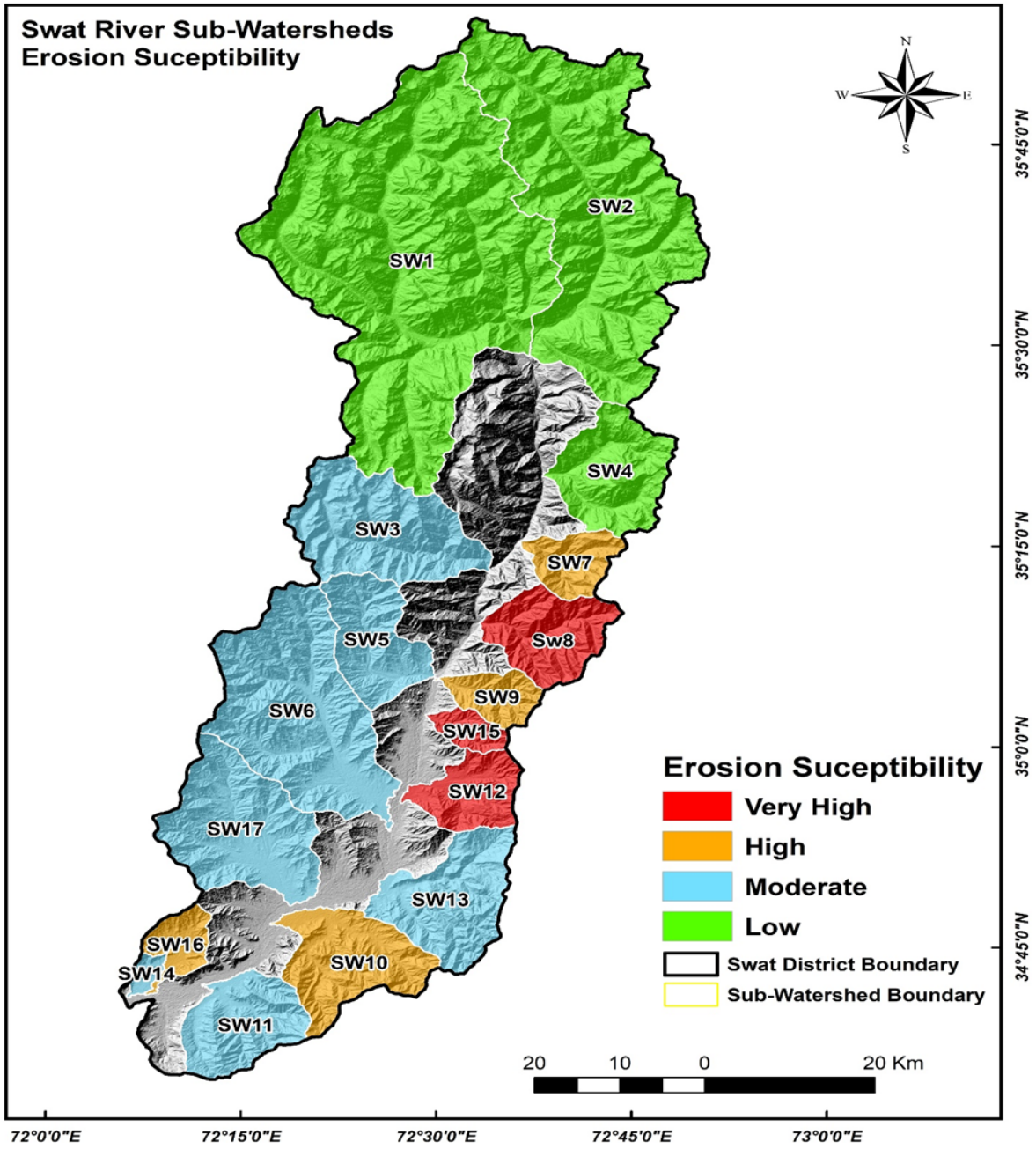

Figure 8

Locations of the Swat River SWs and their susceptibility to erosion based on their CF.

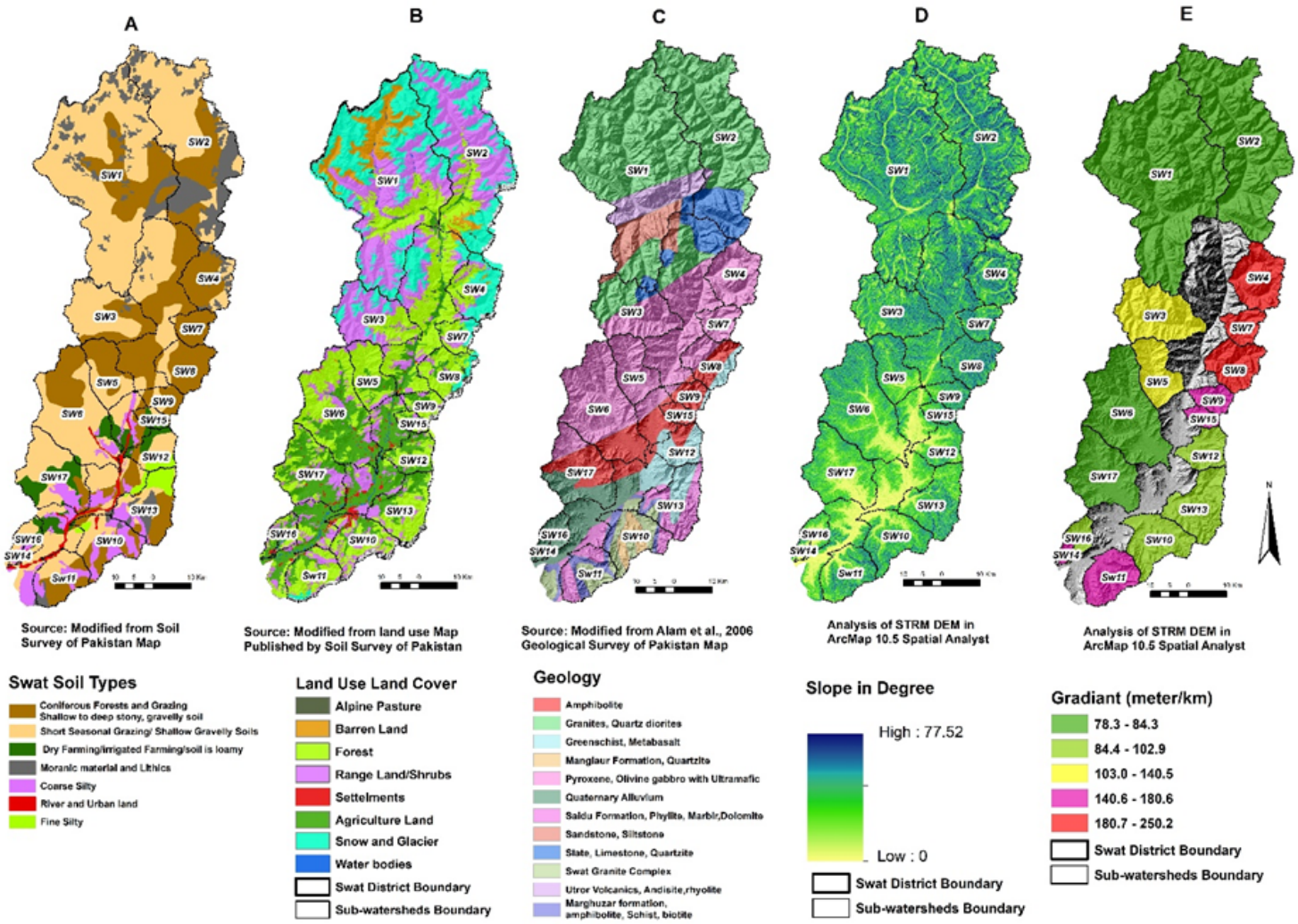

Figure 9

Summary of the **A**soil types, **B** land use, **C** geology and lithology, **D** slope in degrees, and **E** slope gradient for the 17 SWs in the Swat River basin.

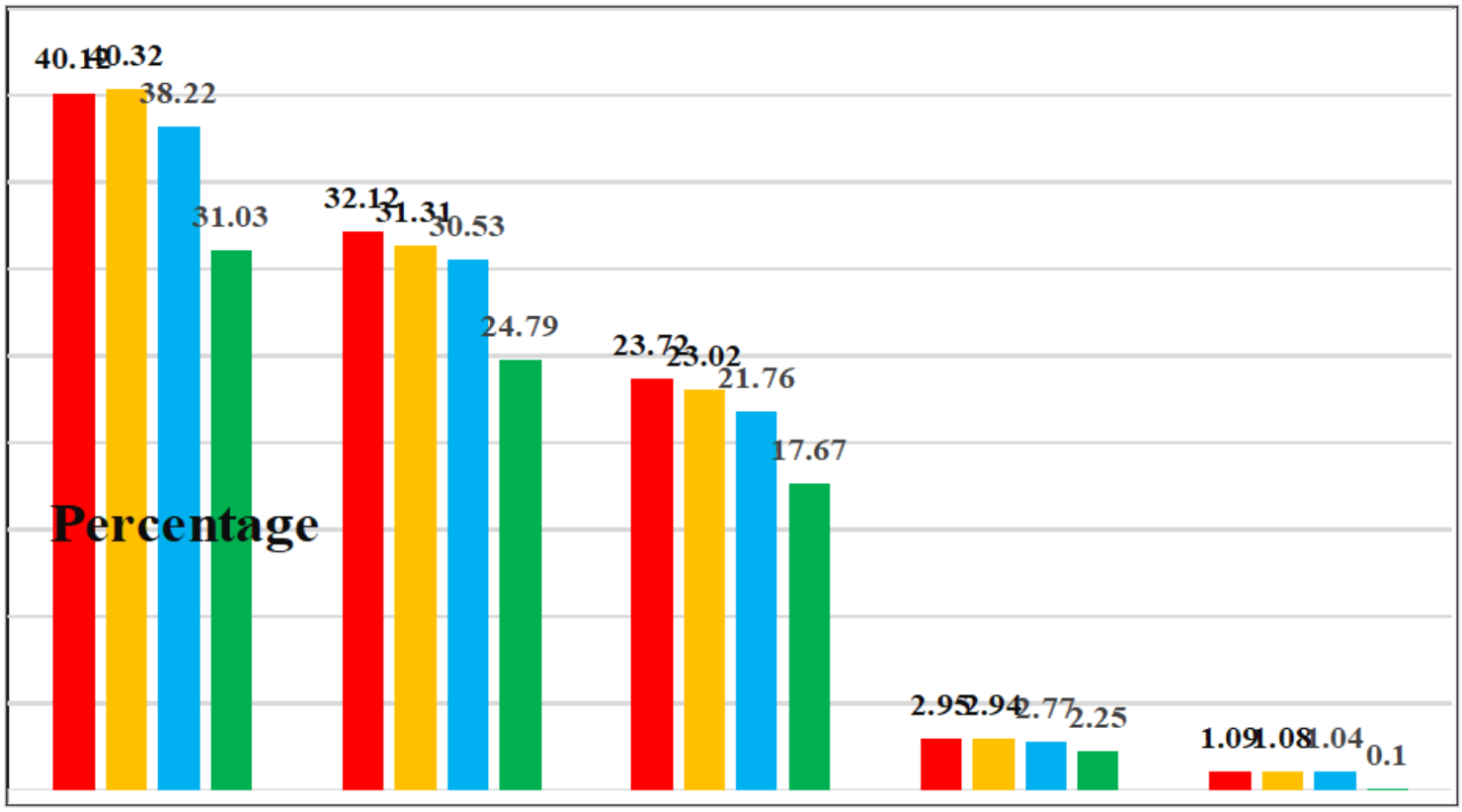

Figure 10

Land use distribution for the Swat River SWs categorized based on their erosion susceptibility.

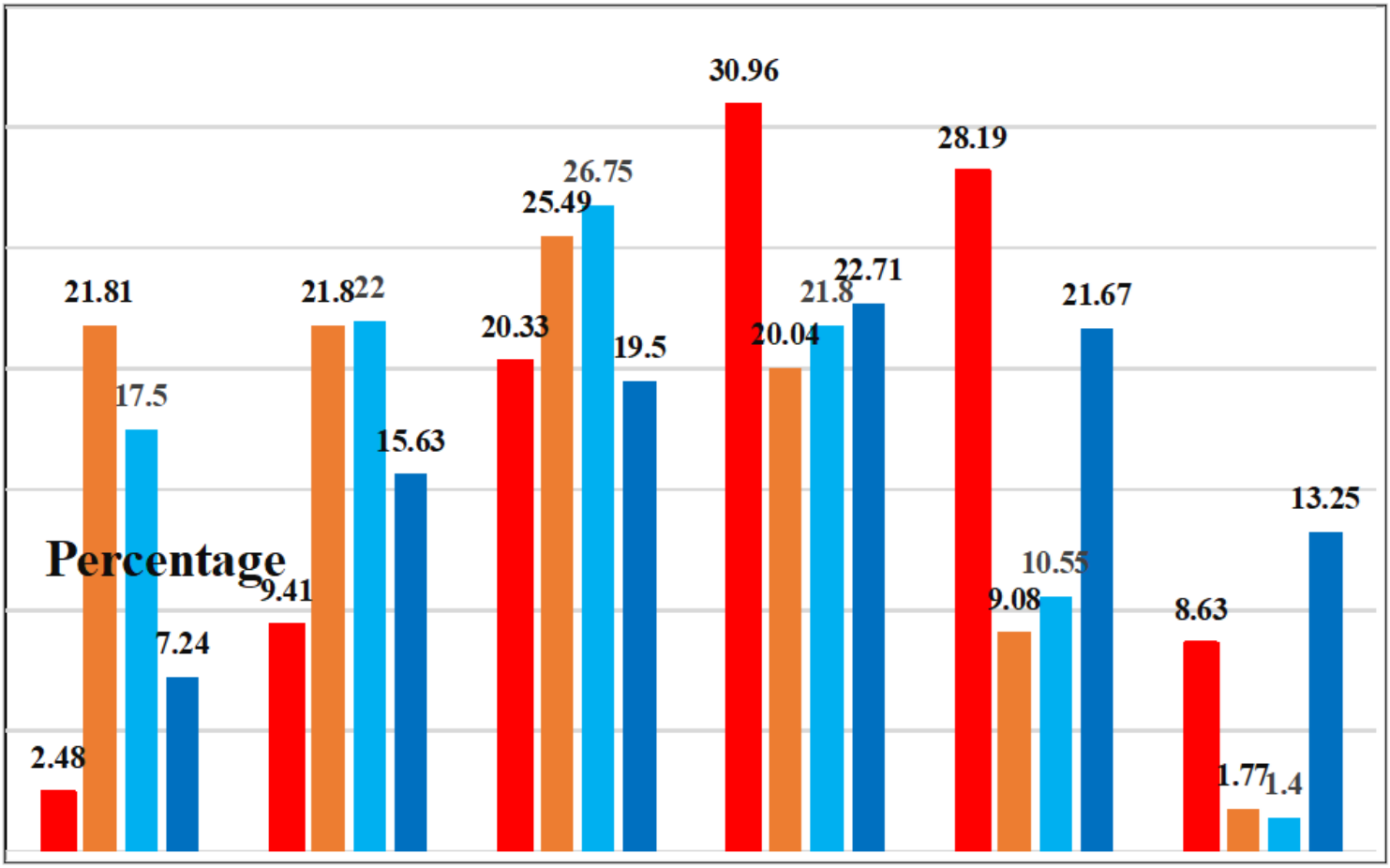

Figure 11

Slope distribution for the Swat River SWs categorized based on their erosion susceptibility.